EXPERIMENTAL INVESTIGATION OF CONFINED MASONRY PANELS WITH OPENINGS UNDER IN-PLANE AND OUT-OF-PLANE LOADS

V. Singhal[1] and Durgesh C. Rai[2]
[1] Doctoral Student, Department of Civil Engineering, Indian Institute of Technology Kanpur, Kanpur, India, singhal@iitk.ac.in
[2] Professor, Department of Civil Engineering, Indian Institute of Technology Kanpur, Kanpur, India, dcrai@iitk.ac.in

ABSTRACT
Load-carrying capacity of masonry walls in the in-plane and out-of-plane directions is affected by presence of openings and type of interface present at the wall edge and the column face. Six half-scaled clay brick masonry wall panels were subjected to a sequence of slow cyclic in-plane drifts and shake table-generated out-of-plane ground motions. Two specimens were regular masonry RC infilled frame with and without window openings. In the other four specimens, confining frame elements were constructed after the masonry wall with one solid wall while the other three had perforations for door and windows bounded by RC confining grid elements on all sides.

Specimens with infill panel demonstrated higher risk of out-of-plane collapse whereas confined masonry wall specimens maintained structural integrity and out-of-plane stability even when severely damaged. The significant improvement in the in-plane lateral load resistance was observed for masonry walls with window openings confined on all four sides; about 70% higher in-plane capacity was observed as compared to regular infill panel with opening. Specimens with appropriate confinement around the openings are able to compensate for the presence of opening and can achieve the performance of the solid masonry wall. Moreover, constructing the masonry wall first and RC elements later, considerably enhance the interaction between masonry walls and frame, which helped delay the failure by controlling out-of-plane deflections even after in-plane drift cycle of 2.1%.

KEYWORDS: confined masonry; seismic behavior; in-plane and out-of-plane loads

INTRODUCTION
Confined masonry wall consists of masonry panel confined with horizontal and vertical reinforced concrete (RC) elements, namely tie-beams and tie-columns. The confined masonry is considerably different from infilled masonry RC frame with respect to *i*) construction methodology, as masonry wall is laid before column and *ii*) load transfer mechanism under gravity and lateral load. Such type of masonry is included in various building codes, such as the Mexico Building Code, the Eurocode, etc. [1]. The structural behavior of confined masonry panels depends on their individual components: the frame is strengthened by the masonry to form a shear resisting element and, in turn, the masonry panel is strengthened by the beneficial containment of the frame. Thus, the coupled system has a high level of stiffness and strength

from the masonry panel and ductility from the surrounding frame. Such construction has been evolved based on its satisfactory performance in past earthquakes [1].

The in-plane performance of confined masonry has attracted considerable interest in seismic research. The summary of experimental studies conducted to understand the in-plane behavior of confined masonry walls in past three decades is presented by Meli et al. [2]. It was observed that confined masonry panels provide fair in-plane shear capacity and ductility and its behavior can be significantly affected by tie-column-to-wall interface, cross-section detailing of tie-column and presence of openings. The openings corresponds to doors and windows of the façade of the building and have negative influence upon seismic resistance of confined masonry walls according to the reconnaissance reports of past earthquake and research evidences [3]. To incorporate deficiencies due to presence of openings appropriate confinement should be provided on all sides of opening which facilitate the development of compression strut in masonry panel for lateral load transfer. Several national standards and technical manuals provide guidelines for the suitable confinement around the door and window openings, however, the efficacy of these confining schemes is still not well known. Although confined masonry construction is commonly recognized as an effective practice, a little effort has yet been made to understand the in-plane and out-of-plane behavior of confined masonry walls with openings.

Moreover, during an earthquake, the masonry panels are subjected to in-plane and out-of-plane loads simultaneously. The out-of-plane load-carrying capacity of these masonry panels may be substantially weakened after being damaged, endangering their overall safety and stability. The extent of damage and likelihood of wall collapse in the out-of-plane direction also depends on presence of openings and connection of masonry panel with adjacent confining elements. Research studies by Tu et al. [4] and Wijaya et al. [5] observed that the wall-frame connection details play a crucial role in the in-plane and out-of-plane behavior of masonry panels. Experimental studies on masonry infilled panels illustrated that an opening of size 20-30% of the panel area may reduce the in-plane stiffness and strength by about 70-80% and 50-60%, respectively [6]. Under out-of-plane loads the presence of opening may cause gross relocation of the yield lines, prevent developing of arching action and induces local effects at corners of opening, thus reduces the overall out-of-plane capacity of panel. Mays et al. [7] observed that the total ultimate out-of-plane resistance of a reinforced concrete panels decreased by up to 60% for opening representing 20% of the panel area.

The present study is an extension of the research in this area and considers dynamic out-of-plane loading of cracked masonry at different damage levels. This paper describes the preliminary results of the experimental research undertaken to study behavior of confined masonry panels with opening under simulated out-of-plane ground motions with prior in-plane damage.

SPECIMEN DETAILS

The experimental work involved six half-scaled wall specimens as shown in Figure 1. The prototype wall was taken to be half-brick thick wall with dimensions of 5 m long by 3 m high, which reduces to 2.5 m × 1.5 m for half-scaled test specimens. All the specimens are designed according to norms of the Mexican code [8]. For 60 mm thick half-scaled wall (slenderness ratio, $h/t = 22.8$), tie-column and tie-beam with 65 mm × 65 mm cross section was provided in all specimens. Two specimens were regular masonry infilled RC frame in which the masonry wall

was built after the RC frame. In other four specimens, the confining (frame) elements were constructed after the masonry wall. The openings for two windows were provided symmetrically in one infill masonry and two confined masonry walls. Both door and window openings were also provided in a confined masonry specimen to study the behavior of wall with asymmetric openings. Two solid masonry walls, one each for infilled masonry and confined masonry was prepared to evaluate the effect of opening. The specimens are designated by alphanumeric symbol as SI, SC, SI-O_{2WA}, SC-O_{2WB}, SC-O_{2WC} and SC-O_{DWB}, where alphabet I and C denote infilled and confined masonry panel, respectively and O signify the masonry panel with openings. The subscript W and D represents type of opening, i.e., window and door opening, respectively and numeric symbol corresponds to number of window openings. The subscript A, B and C signify the type of confinement scheme used to enclose the opening as follows:

A. Only lintel beam provided over the opening.
B. Opening confined on all sides with tie-columns extending from bottom to top tie-beam.
C. Opening confined on all sides with continuous sill and lintel band.

The details of the geometry and reinforcement are summarized in Figures 1 and 2. The masonry panel of all specimens were laid in stretcher bond using solid burnt clay bricks. Generally, prototype masonry has a mortar joint thickness in the range of 10 mm - 12 mm, so to satisfy the length ratio of the models, they should have had a mortar joint thickness of 5 mm - 6 mm. However, due to practical difficulties, an average thickness of 7 mm was obtained for all joints.

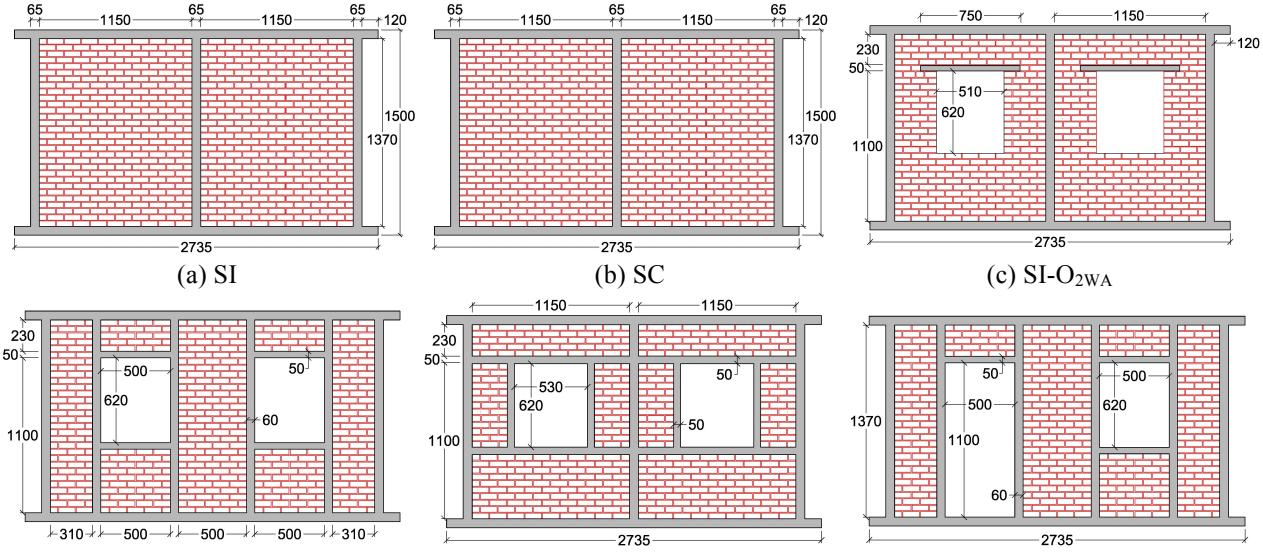

Figure 1: (a) – (f) Details of masonry wall specimens

MATERIAL PROPERTIES

Specially made half-scaled burnt clay bricks (120.4 mm × 61.8 mm × 38.5 mm) and a lime-cement mortar mix of 1:1:6 proportion (cement: lime: sand) was used for the masonry panels. The water-binder ratio of 0.85 was used to obtain workable mortar in a hot and dry climate. Micro-concrete of mix proportion 0.50:1:2.75 (water: cement: aggregate) was used in RC members of all specimens. The average compressive strength of the bricks was found to be

33.9 MPa. Masonry prisms of five bricks tall were made during construction of brick wall and were moist cured for 28 days before testing. The average reference properties of material units and brick assemblages obtained from different tests for all specimens are summarized in Table 1. For all wall specimens steel wires of 6 mm and 3 mm diameter were used as longitudinal and transverse reinforcement in tie-beams and columns, respectively.

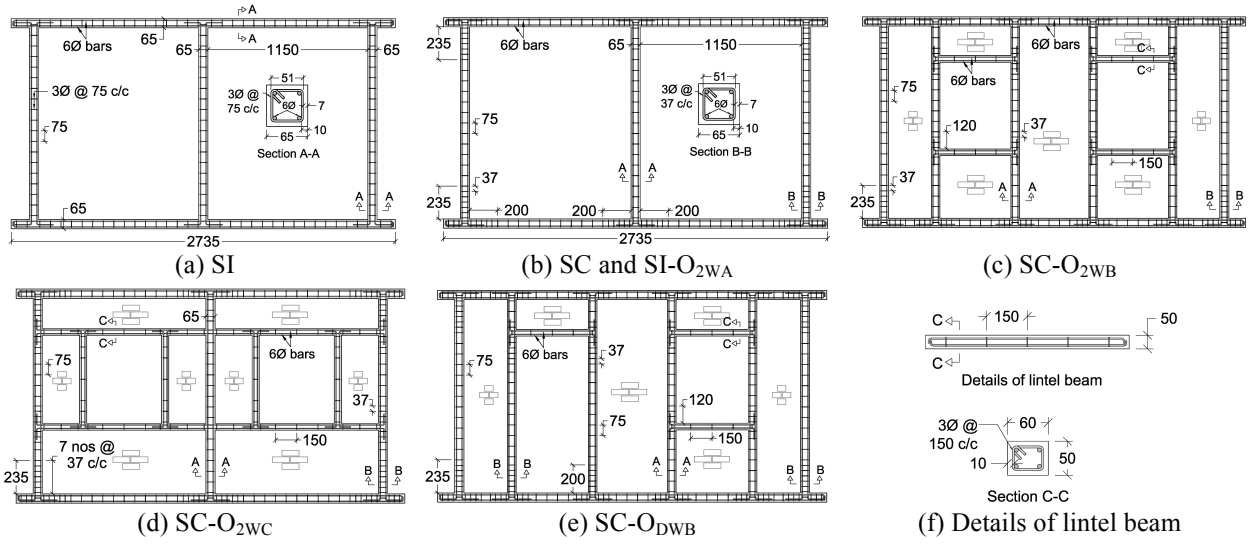

(a) SI (b) SC and SI-O_{2WA} (c) SC-O_{2WB}

(d) SC-O_{2WC} (e) SC-O_{DWB} (f) Details of lintel beam

Figure 2: (a) – (f) Reinforcement details of RC members in masonry wall specimens

Table 1: Average properties of material used in model specimen

Confinement Schemes	Properties (MPa)[§]				
	Mortar compressive strength, f_j	Masonry Prism		Micro concrete	
		Compressive Strength, f'_m	Elastic Modulus, E_m	Compressive Strength, f'_{ck}	Tensile Strength, f_t
SI	7.2 [15]	10.3 [10]	2705 [27]	30.1 [16]	3.0 [28]
SC	7.1 [25]	8.8 [19]	3845 [29]	33.1 [14]	4.0 [10]
SI-O_{2WA}	6.0 [7]	7.5 [17]	2628 [48]	30.6 [16]	3.4 [8]
SC-O_{2WB}	5.7 [14]	7.8 [15]	2854 [41]	30.3 [13]	3.3 [16]
SC-O_{2WC}	7.3 [19]	8.5 [22]	3927 [48]	34.1 [13]	4.0 [8]
SC-O_{DWB}	5.2 [19]	7.9 [11]	3026 [37]	30.3 [13]	3.3 [16]

[§] Figures in bracket [ ] indicate percent coefficient of variation (COV).

ARTIFICIAL MASS SIMUALTION

For a reliable correlation study with the prototype, one of the most important considerations is the appropriate modeling as per relevant similitude relations. The required similitude relations to be satisfied for adequate dynamic modeling are listed in Table 2. Simulation of forces includes both gravitational and inertial types, which can be achieved by adding structurally ineffective lumped masses [9]. For out-of-plane ground motions, the inertia forces are predominant forces on masonry wall panels and may cause instability in the walls, especially in slender walls with large height-to-thickness ratios. In this particular case, the artificial mass should also be

distributed throughout, as the resulting inertia forces are uniformly distributed. The artificial mass, Δm which needs to be added can be given by the following relation [10].

$$\Delta m = m_m \left(\frac{1}{S_l} - 1 \right) \tag{1}$$

where, m_m is the mass of unit volume of the model brick masonry. Consequently, for half-scaled model bricks, the additional mass added for each brick in the wall is equal to the mass of that brick. Since the mass of a typical brick was approximately 0.435 kg, a lead block with a diameter of 60 mm, a height of 28 mm, and a weight of 0.865 kg, was attached to the wall in order to serve as artificial mass for two bricks. These lead blocks were arranged in a regular grid pattern on both faces of the wall to eliminate any eccentric loading in the out-of-plane direction.

Table 2: Similitude requirements for dynamic shake table test of half-scaled model

Parameter	Scale factor	Replica model value
Length scale ratio, S_l	l_m/l_p	1/2
Modulus ratio, S_E	E_m/E_p	1
Acceleration scale ratio, S_a	a_m/a_p	1
Time scale ratio, S_t	t_m/t_p	$1/\sqrt{2}$
Frequency scale ratio, S_ω	ω_m/ω_p	$\sqrt{2}$

Subscript notation: m = model; p = prototype

TEST SETUP

The unique testing method developed by Komaraneni et al. [11] was used in this study, which involved successive applications of out-of-plane and in-plane loading, so that there was no need to move the specimen for the repeated cycles of loading in in-plane and out-of-plane directions. The test setup for the out-of-plane and in-plane loading are shown in Figures 3 & 4. Few modifications were made from previous test set-up to improve the stiffness of lateral supports in the out-of-plane direction and fixity of test wall for overturning and sliding during in-plane loads. A 1.8 m × 1.2 m servohydraulic-driven uniaxial shake table was used for the out-of-plane loading [12]. For in-plane loads, four bars with a diameter of 20 mm were used to connect both ends of the top beam with a 250 kN servohydraulic actuator. The desired boundary conditions of diaphragm flexibility and deformations of the perpendicular walls were achieved by providing a sufficient number of lateral supports as shown in Figures 3 and 4. The lateral supports provided on both sides of the wall were braced at the top to ensure sufficient torsional restraint to the RC beams and masonry walls during both in-plane and out-of-plane loading. The in-plane supports were attached to the strong-reaction floor to transfer overturning loads generated during the in-plane loading without overstressing the shake table bearings. In order to simulate gravity loads on the masonry panels, a vertical precompression force of 0.10 MPa was applied over the wall specimen with the help of a flexible wire rope arrangement.

For out-of-plane tests, 20 accelerometers were used: 18 were attached to the wall, one was fixed to the shake table and another was placed at the centre of top tie-beam. Four load cells were kept to measure variations in the vertical compressive load on the wall during testing. For both in-

plane and out-of-plane tests, sufficient numbers of linear variable differential transducers (LVDT) and wire potentiometers were provided to monitor the wall displacement. A high-performance data acquisition system was used to collect data from sensors at a rate of 200 samples per second.

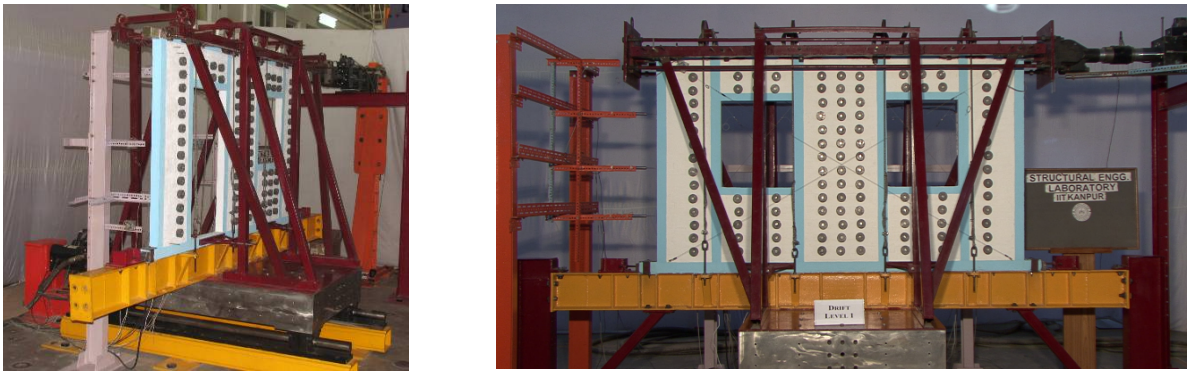

(a) (b)

Figure 3: Test setup for (a) out-of-plane loading and (b) in-plane loading

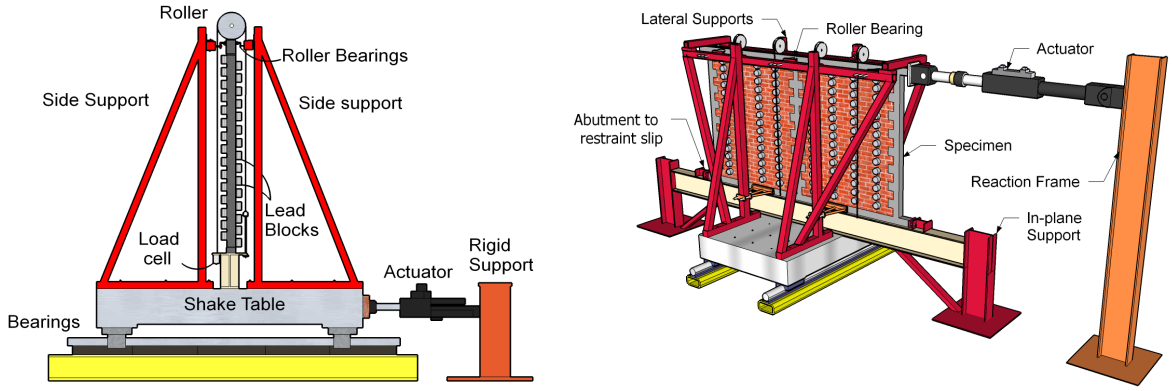

(a) (b)

Figure 4: Schematic showing various components of the test setup for (a) out-of-plane and (b) in-plane loading

LOADING HISTORY

The N21E component of the 1952 Taft earthquake was chosen for the out-of-plane target ground motion, with a PGA of 0.156g. The first 30 s of ground motion was considered for the simulation (Figure 5a), which included the strong motion portion and the time axis of the accelerogram was compressed by a factor of $1/\sqrt{2}$ to satisfy the dynamic similitude relations.

The 5% damped response spectrum of the Taft ground motion input was compared with the scaled design response spectrum specified in the IS 1893 [13] for a design earthquake in Zone V (PGA = 0.36g), and a reasonable match was observed when the Taft motion was scaled to make its PGA equal to 0.40g, as shown in Figure 5b. Also, the response spectra of the recorded Taft motion at the top of the shake table after appropriate tuning corresponded well with that of the original ground motion scaled to 0.4g as shown in Figure 5b & 5c. This ground motion is referred as Level V motion. Similarly, the Taft motion is scaled to a corresponding Zone II, III and IV of Indian seismic code and referred as Level II, III and IV motions, respectively. A low-

intensity white noise test (0.05g) was also conducted to investigate the change in the stiffness properties of the specimen after each cycle of the Taft earthquake motion. In-plane loading consists of displacement controlled slow cycle as per ACI 374.1-05 [14]. This loading history consists of gradually increased storey drifts (displacements) of 0.20%, 0.25%, 0.35%, 0.50%, 0.75%, 1.00%, 1.40%, 1.75% and 2.20%. Each cycle was repeated for three times at each drift ratio. The test was discontinued when either the specimen failed or suffered severe damage before the maximum drift level of 2.20% was reached.

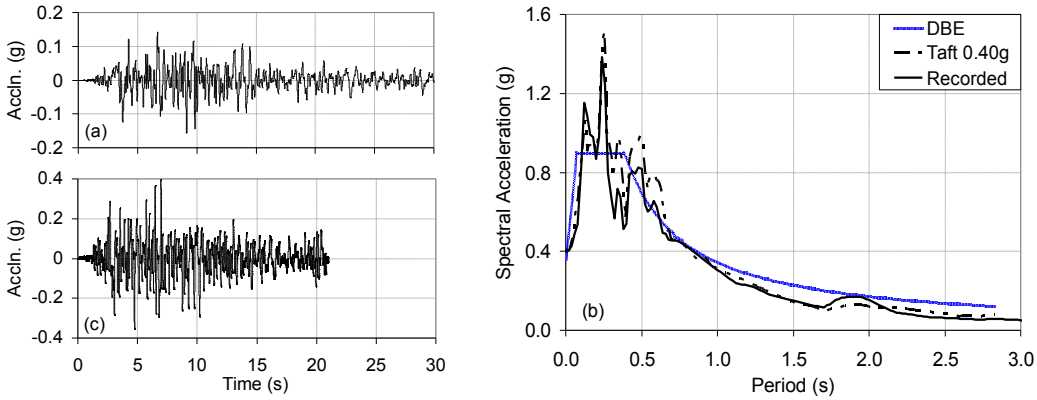

Figure 5: (a) TAFT N21E ground motion (b) Comparison of scaled response spectra of DBE (Design Basis Earthquake), original TAFT motion upscaled to 0.4g and recorded TAFT motion at table top surface. (c) Scaled TAFT motion recorded at shake table top surface

TEST PROCEDURE

After safely mounting the specimen on the shake table, forced vibration tests were performed to obtain the initial dynamic characteristics of the specimens. The load test started with the out-of-plane shake table motions consisting of a series of incremental Taft motions from Level I to Level V, with the white noise tests in between. After the completion of this out-of-plane loading schedule, the specimen was subjected to quasi-static in-plane cyclic loading. The in-plane cyclic loading was continued until cracks were visible, which was observed at the 0.50% drift cycle for all specimens. After this drift level, the second cycle of out-of-plane loading was applied which consisted of Level V Taft motion only, preceded and followed by white noise loading. The second cycle of in-plane loading was performed (drift ratio 0.75%) and an alternate process of out-of-plane and in-plane loading was continued until the specimen failed as shown in Figure 6.

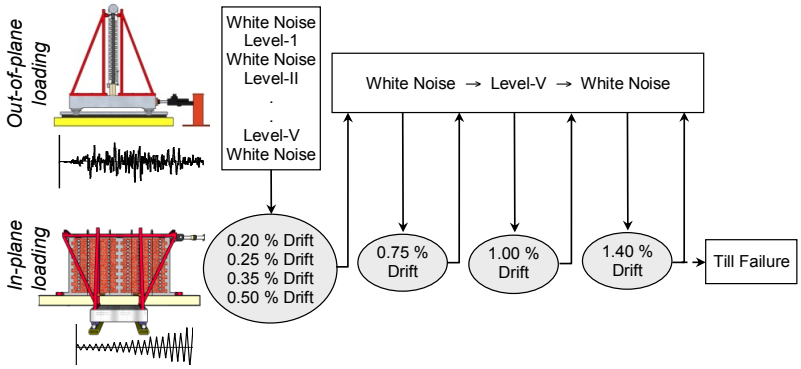

Figure 6: Summary of test procedure and loading sequence

OBSERVED BEHAVIOR

A majority of the cracks were formed due to the in-plane loading, while not many new cracks were observed during the out-of-plane loading. In subsequent loading cycles, the cracks formed at the initial stages of in-plane loading widened, and energy dissipation was mainly due to the sliding of masonry blocks along bed joints. In solid masonry wall specimens (SI and SC), the diagonal bed joint crack propagated from one load corner to another along with horizontal sliding, which eventually led to the formation of plastic hinges at the column ends and subsequent failure of exterior tie-column at higher drift level. The failure patterns of all six specimens are illustrated in Figures 7 and 8. The specimens SI and SI-O_{2WA} with infill masonry showed separation of masonry wall with RC tie-beams and tie-columns even at in-plane drift level of 0.5%. However, confined masonry specimens did not experienced any such separation till the drift cycle of 1.75%.

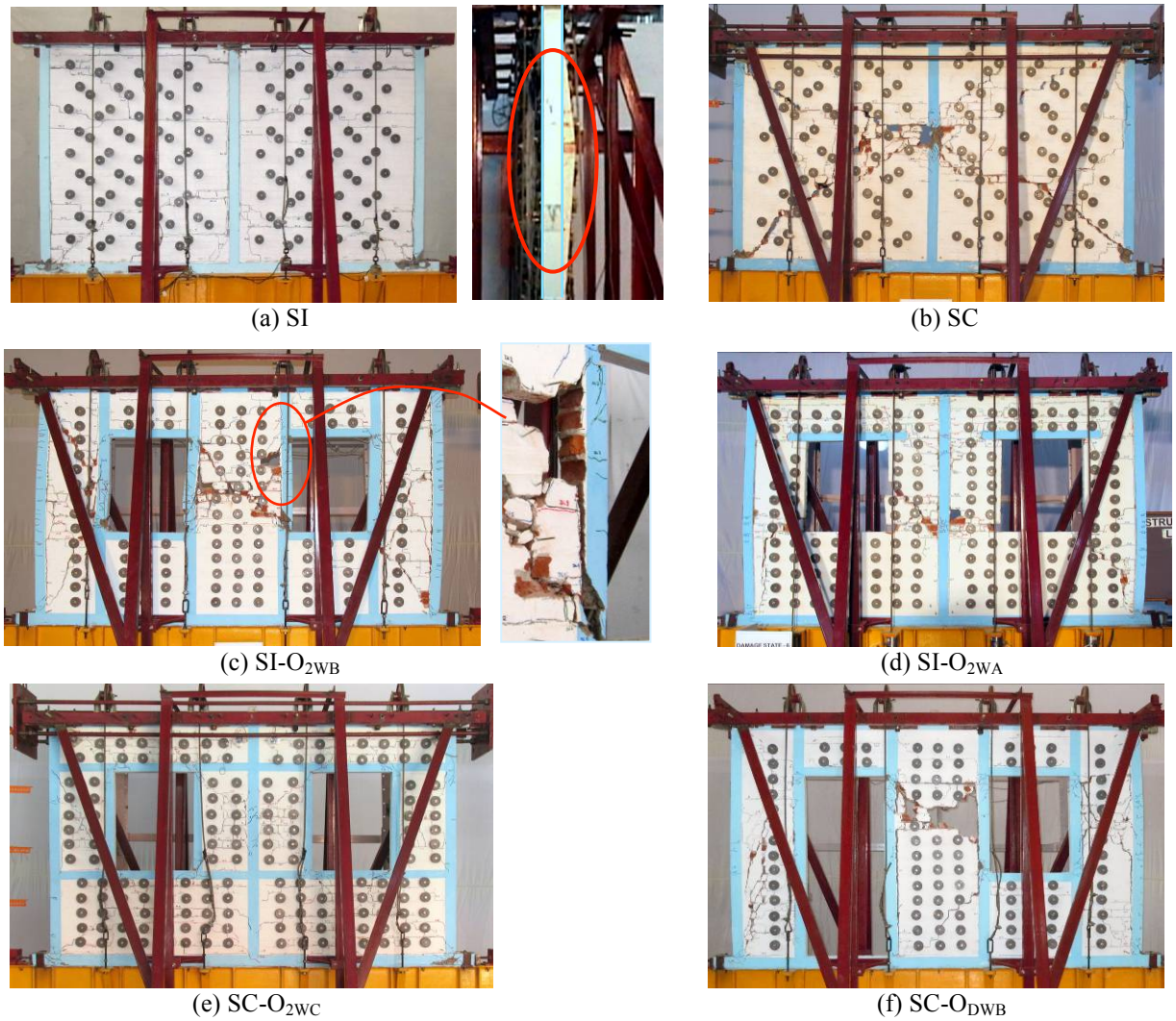

(a) SI (b) SC

(c) SI-O_{2WB} (d) SI-O_{2WA}

(e) SC-O_{2WC} (f) SC-O_{DWB}

Figure 7: Cracking pattern after last in-plane damage (drift) cycles for specimen (a) SI with arching phenomenon under out-of-plane shake table motion, (b) SC, (c) SC-O_{2WB} with enhanced interaction between wall and RC confining element, (d) SI-O_{2WA}, (e) SC-O_{2WC} and (f) SC-O_{DWB}

Masonry walls with opening experienced the rocking of masonry piers under in-plane loads and with subsequent loading cycles excessive crushing of bricks was observed at piers ends (toe and heel). The specimen with only lintel beam (SI-O_{2WA}) developed first crack at the edges of opening and the masonry around opening become highly vulnerable to collapse during out-of-plane loading following the 1.75% in-plane drift cycles. The performance of specimen SI-O_{2WA} dictates the necessity of appropriate confinement around openings. Specimens with confinement on all sides of opening significantly improved the load carrying capacity of masonry wall in range of 40% - 70% as compared to SI-O_{2WA}. Even the specimen with large door opening (SC-O_{DWB}) did not experience any catastrophic failure. However, the specimens with confinement scheme B suffered rocking of masonry pier and severe crushing/cracking of bricks and tie-columns on the sides of opening at higher drift levels. The specimen with continuous sill and lintel band (SC-O_{2WC}) showed uniformly distributed cracks formed in a stepped manner with sliding taking place at multiple bed joints and no major cracks were observed in piers, spandrels and confining elements even after 2.2% in-plane drift cycle (Figures 7e and 8e).

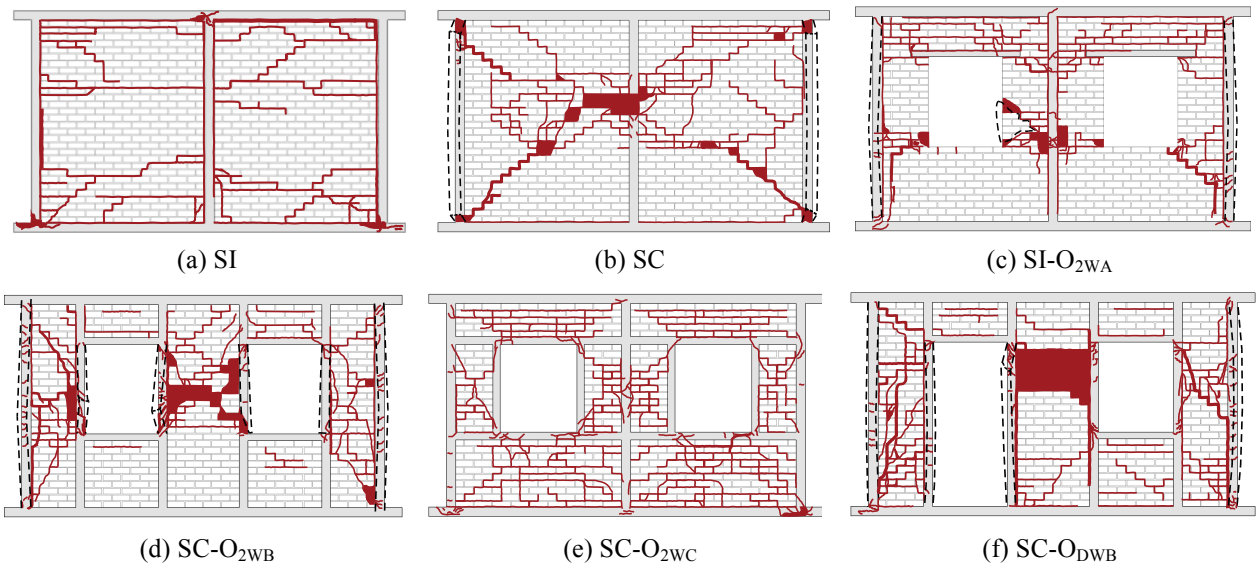

(a) SI (b) SC (c) SI-O_{2WA}

(d) SC-O_{2WB} (e) SC-O_{2WC} (f) SC-O_{DWB}

Figure 8: Comparison of cracking patterns for all specimens after last in-plane damage cycle

The specimens with infilled masonry showed significant out-of-plane deflection and arching after being subjected to a 1.75% in-plane drift and were on the verge of possible collapse due to overturning of wall panels (Figure 7a). However, in confined masonry walls relatively smaller out-of-plane deflections were observed even after 1.75% in-plane damage cycle. The confined masonry construction strengthened the wall to tie-column interaction and prevents the early separation of masonry wall with tie-columns. The failure of wall-to-tie-column connection in confined masonry specimens was due to rupture of bricks at the interface as shown in Figure 7c. The test was stopped after 1.75% and 2.20% drift cycle for solid wall and walls with opening due to either fracture of longitudinal reinforcing bar in the tie-columns or extensive cracking of masonry, respectively.

RESULT AND DISCUSSION

The variation of equivalent uniform pressure (calculated from observed inertia forces) and average peak out-of-plane displacement at mid-height in each panel with in-plane drift (damage)

is shown in Figures 9a and 9b, respectively. The equivalent uniform pressure was calculated by multiplying average of peak acceleration at each location (18 accelerometers mounted on wall) with the total mass of wall and then divided by the wall area. All specimens experienced relatively small variations in uniform pressure during the out-of-plane motion. As observed from Figure 9a, the specimen SI reached its peak uniform pressure in an undamaged state and once damage was introduced, the acceleration response decreased with continued in-plane damage except after 1.4% in-plane drift. However, in the confined masonry specimens (SC, SC-O_{2WB}, SC-O_{2WC} and SC-O_{DWB}) nearly constant uniform pressure was observed for all in-plane damage levels. The increase in uniform pressure in specimen SI-O_{2WA} after few in-plane drift cycles was may be due to higher local acceleration resulted from rocking of damaged masonry fragment.

Specimen SI with infilled masonry showed continuous increase in out-of-plane deflection with in-plane damage and was likely to collapse after 1.75% drift cycle. Conversely, the maximum out-of-plane displacement in specimen SC remains fairly invariable with in-plane damage (Figure 9b). This indicates that the observed out-of-plane instability was primarily due to excessive deflections and not governed by the accelerations (inertia forces). The confined masonry walls behaved more like a shear wall with boundary elements and enhanced integrity of wall panel to columns helped reduce the likelihood of out-of-plane instability. The specimen with window openings did not experience large out-of-plane displacement even after 1.75% in-plane drift cycle. However, due to major damage of masonry around openings in specimen SI-O_{2WA} and crushing of bricks in piers in SC-O_{2WB}, significant displacement was observed in these specimens during out-of-plane loading following 2.20% in-plane drift. On contrary, the specimen with continuous lintel and sill band showed least variation in out-of-plane deflections even beyond 2.20% drift cycle and behaved similar to shear wall with openings.

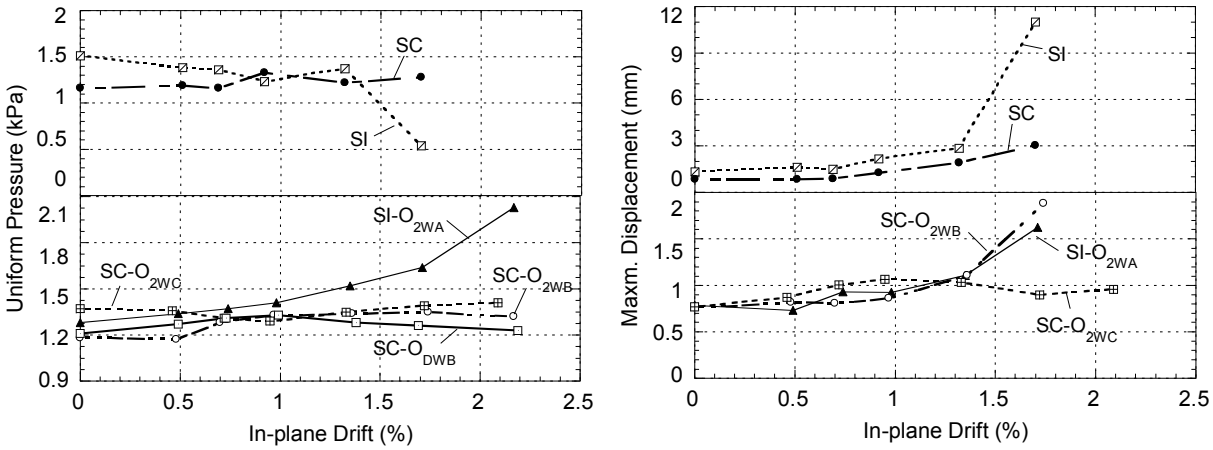

Figure 9: (a) Variation of peak uniform acceleration and (b) out-of-plane displacement with in-plane drift/damage

Before and after each out-of-plane ground motion excitation, a white noise test run was performed to determine the natural frequencies of vibration. These tests often showed a decrease in the natural frequencies after each in-plane damage state, indicating the softening of the specimen due to accumulated damage during the test. The fundamental natural frequencies of all specimens at undamaged state and at the end of the test are listed in Table 3. The undamaged

specimens had initial fundamental natural frequencies of 13.5 Hz and 15.1 Hz for specimens SI and SC, respectively. The slight increase in the natural frequencies of confined specimens as compared to infilled masonry may be due to the increase in stiffness on account of enhanced interaction at wall-to-tie-column interface. As shown in Table 3, the solid masonry infill specimen SI experienced maximum reduction of 76% in the fundamental frequencies before failure, however, only 14% reduction was observed in specimen SC. Among the specimens with window openings, the specimen SC-O_{2WC} showed least change in natural frequency, i.e., 10% of undamaged specimen.

Table 3: Comparison of fundamental frequency at initial and conclusion of test for all specimens

Damage state	Fundamental natural frequency (Hz)					
	SI	SC	SI-O_{2WA}	SC-O_{2WB}	SC-O_{2WC}	SC-O_{DWB}
Undamaged	13.5	15.1	15.2	16.2	16.0	15.4
At the end of test	3.2	13.0	12.6	11.6	14.3	15.0

The in-plane load-displacement hysteretic response for all specimens is shown in Figures 10. The observed in-plane response in terms of ultimate load, effective stiffness and hysteretic energy dissipated are listed in Table 4. The effective stiffness was estimated by idealizing the load-deformation plot with a bi-linear curve. As observed from Figure 10a & 10b the specimen SI with masonry infilled RC frame showed relatively pinched hysteretic behaviour as compared to confined masonry specimen SC. The enhanced interaction at the wall-to-tie-column interface due to confined masonry construction significantly improves the energy dissipation capacity of wall as compared to infilled masonry.

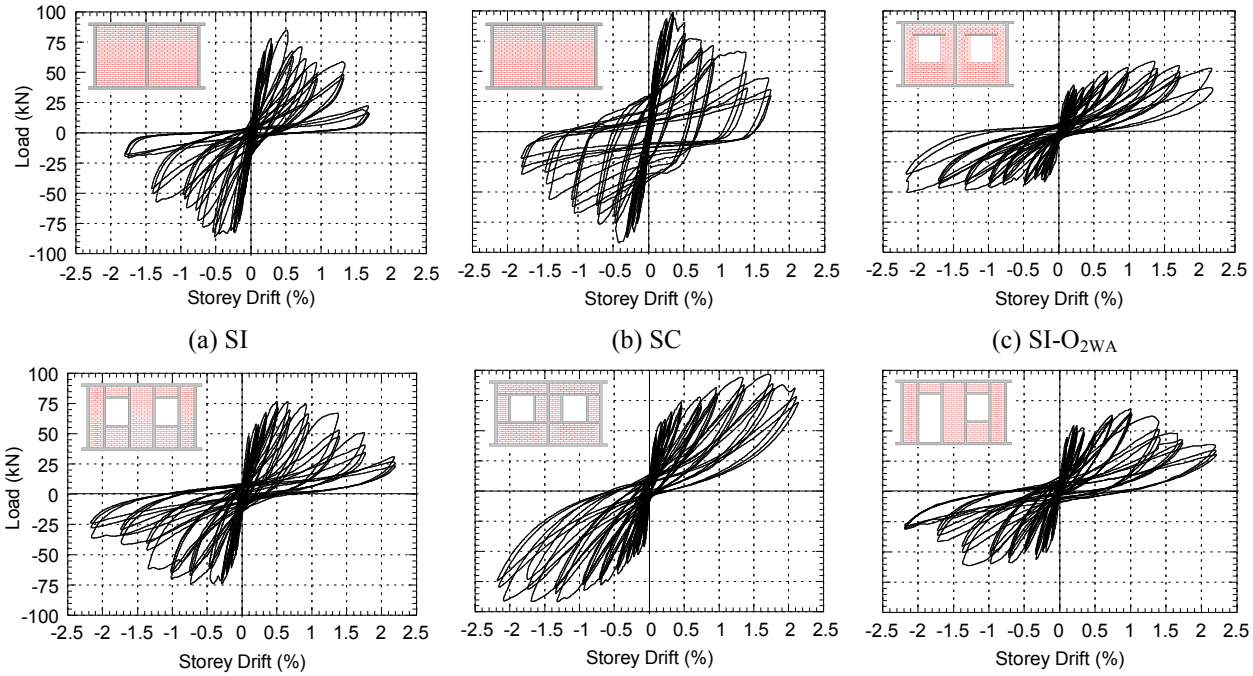

(a) SI (b) SC (c) SI-O_{2WA}

(d) SC-O_{2WB} (e) SC-O_{2WC} (f) SC-O_{DWB}

Figure 10: Hysteretic behavior of specimens

The envelope backbone curves for wall specimens with window opening were compared with solid masonry walls in Figure 11a. The envelope backbone curve shown in Figure 11a was obtained by joining the point of peak displacement during the first cycle of each increment of loading as indicated in ASCE/SEI 41-06 [15] and then taking the mean of both positive and negative backbone curves. As observed from Table 4 and Figure 11a, confinement configuration in specimen SC-O_{2WB} and SC-O_{2WC} considerably improves the strength and energy dissipation potential (> 40%) as compared to specimen with only lintel beam (SI-O_{2WA}). Moreover, provision of continuous sill and lintel band significantly enhance the strength and deformability of wall specimen. Both confinement configuration B and C were able to regain for the deficiency due to the presence of openings. To illustrate the stiffness degradation occurring between different loading sequences, cycle stiffness (K_i) as defined by Komaraneni et al. [11] was estimated for each specimen as shown in Figure11b. It can be seen that cyclic stiffness steadily declined with each loading cycle and with the resulting accumulated damage. All specimen followed similar trends for stiffness degradation with in-plane drift cycle, however, confined masonry specimens showed higher initial stiffness in the range of 30 – 70% as compared to infilled frame specimen.

Table 4. Summary of observed response for all specimens

Specimen	Ultimate Load, R_u (kN)	Displacement at Peak Load (mm)	Effective Stiffness, K_e (kN/mm)	Cumulative Energy Dissipated (kN m/m^3)
SI	85.5	7.7	31.2	36.5
SC	93.0	4.9	42.4	81.0
SI-O_{2WA}	52.4	20.2	16.4	35.1
SC-O_{2WB}	74.7	10.5	31.0	51.1
SC-O_{2WC}	92.7	23.0	17.7	53.2
SC-O_{DWB}	63.0	17.8	25.8	44.7

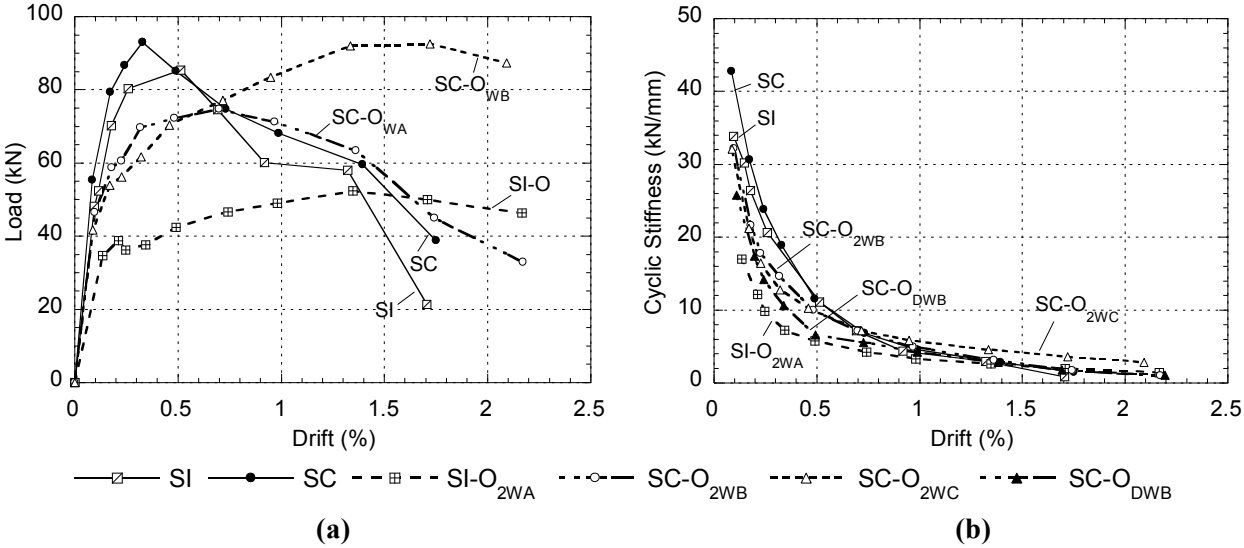

Figure 11. Comparison of observed responses for all specimens (a) Envelope value of load versus story drift (b) cyclic stiffness against story drift

CONCLUSION

The study was concerned with the evaluation of out-of-plane response of confined masonry walls with opening when damaged due to in-plane forces. Six half-scaled specimens of large slenderness ratio (h/t = 22.8) were observed to maintain structural integrity and out-of-plane stability under the design level out-of-plane inertial forces even in the damaged state caused by in-plane drifts in the excess of 1%. Confining opening on all sides with RC elements clearly improved both in-plane and out-of-plane response and were able to recover for deficiencies due to opening. The masonry wall with continuous sill and lintel band performed superior than other confinement configurations and assisted in uniform distribution of cracks which led to significantly enhanced strength and deformability. Under lateral load, confined masonry walls acted as a shear wall and due to the composite action between wall and the tie-column, the out-of-plane failure was delayed and it could safely sustain large in-plane drifts upto 1.75%. However, RC frame with infill masonry showed the separation of wall panel at its interface with the framing element at in-plane drifts as low as 0.5%, which led to excessive out-of-plane deflection and increased risk of dislodgement from the frame.

ACKNOWLEDGEMENTS

The financial support provided by the Ministry of Human Resource Development, Government of India is gratefully acknowledged. The authors sincerely appreciate the assistance received from the staff of the Structural Engineering Laboratory of the Indian Institute of Technology Kanpur.

REFERENCES

1. Brzev, S. (2008). "Earthquake-Resistant Confined Masonry Construction" National Information Center of Earthquake Engineering, Indian Institute of Technology Kanpur, India.
2. Meli, R., Brzev, S., Astroza, M., Boen, T., Crisafulli, F., Dai, J., Farsi, M., Hart, T., Mebarki, A., Moghadam, A. S., Quiun, D., Tomazevic, M. and Yamin, L. (2011). "Seismic Design Guide for Low-Rise Confined Masonry Buildings." World Housing Encyclopedia, EERI and IAEE, [Online], Available: www.confinedmasonry.org/risk-management-solutions-supports-network/design-guideline-working-group [1 Nov. 2011].
3. Yáñez, F., Astorza, M., Holmberg, A. and Ogaz, O. (2004). Behavior of Confined Masonry Shear Walls with Large Openings. 13th World Conference on Earthquake Engineering, Vancouver, Canada.
4. Tu, Y. H., Chuang, T. H., Liu, P. M., and Yang, Y. S. (2010). "Out-of-Plane Shaking Table Tests on Unreinforced Masonry Panels in RC Frames." Engineering Structures, 32, 3295-3935.
5. Wijaya, W., Kusumastuti, D., Suarjana, M., Rildova and Pribadi, K. (2011). "Experimental Study on Wall-Frame Connection of Confined Masonry Wall." Procedia Engineering, 14, 2094-2102.
6. Liauw T. C., 1979. "Tests on multi-story infilled frames subject to dynamic lateral loading." ACI Journal, 76, 551–563.
7. Mays, G. C., Hetherington, J. G., and Rose, T. A. (1998). "Resistance-Deflection Functions for Concrete Wall Panels with Openings." Journal of Structural Engineering, 124(5), 579–587.
8. NTC-M. (2004). "Commentary Technical Norms for Design and Construction of Masonry Structures." Mexico D.F.
9. Mills, R. S., Krawinkler, H., and Gere, J. M. (1979). "Model Tests on Earthquake Simulators: Development and implementation of experimental procedures." Report No. 39, The John A. Blume Earthquake Engineering Center, Stanford University, CA.
10. Tassios, T.P. (1992). "Modelling of Structures Subjected to Seismic Loading." Small Scale Modelling of Concrete Structures, F.A. Noor and L. F. Boswell, eds., Elsevier Applied Science, New York, 229-271.

11. Komaraneni, S., Rai, D. C. and Singhal, V. (2011). “Seismic Behavior of Framed Masonry Panels with Prior Damage when Subjected to Out-of-Plane Loading.” Earthquake Spectra, 27:4, 1077-1103.
12. Sinha, P., and Rai, D. C. (2009). “Development and Performance of Single-axis Shake Table for Earthquake Simulation.” Current Science, 96:12, 1611–1620.
13. BIS. (2002). “IS 1893: Indian Standard Criteria for Earthquake Resistant Design of Structure, Part 1: General provisions and buildings.” Bureau of Indian Standards, New Delhi, India.
14. ACI. (2006). “ACI 374.1-05: Acceptance Criteria for Moment Frames Based on Structural Testing and Commentary.” American Concrete Institute, Farmington Hills, MI.
15. ASCE. (2007). “ASCE/SEI 41-06: Seismic rehabilitation of existing buildings.” American Society of Civil Engineers, Reston, VA.